

Fig. 1 Pressure distribution

forementioned method (within 3%) for both  $\gamma = \frac{7}{5}$  and  $\frac{5}{3}$ . Once the pressure distribution is known the heat transfer can be computed in the previously indicated manner.

The aforementioned theories are compared with the experimental pressure and heat transfer distributions obtained on a flat faced circular cylinder in helium at  $M \sim 11$  on Figs. 1 and 2. In applying Oguchi's method a value of  $a/a^* = 0.90$  was chosen. If the actual value of  $a$  were used, its deviation from the assumed value would be a maximum of  $\pm 5\%$ . Also examining the equation for  $a$ , it is seen that the slope of the theory on Fig. 1 would increase, but this change would be in poorer agreement with experiment than the one presented. The blast wave solution without the correction for finite freestream pressure is also presented on Fig. 1. For the extension of Cheng's theory, the drag coefficient was taken to be equal to 1.71. Examining both the pressure and heat transfer data, it is seen that only the present extension of Cheng predicts the correct variation of the data. Cheng's method was derived in the limit of small  $\epsilon$ , and the present comparison is for helium with  $\epsilon = \frac{1}{4}$ . A first-order correction for the effect of finite  $\epsilon$  will tend to raise the overall level of the predicted pressure distribution. This correction will decrease the accuracy of the theoretical pressure distribution but improve the agreement of the theory with the heat transfer results. Although the two theories are in poor agreement with the heat transfer results, they are as good as or better than various other theories that require a pressure distribution obtained from experimental data (see Ref. 3).

#### References

- Cheng, H. K., Hall, J. G., Golian, T. C., and Hertzberg, A., "Boundary-layer displacement and leading-edge bluntness

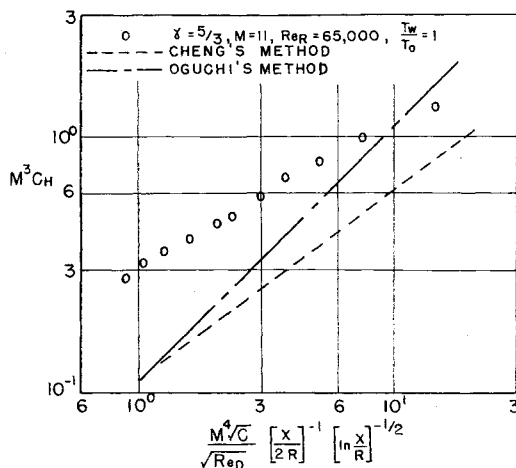


Fig. 2 Heat transfer distribution

effects in high-temperature hypersonic flow," J. Aerospace Sci. 28, 353-381 (1961).

<sup>2</sup> Oguchi, H., "The blunt-leading-edge problem in hypersonic flow," AIAA J. 1, 361-368 (1963).

<sup>3</sup> Horstman, C. C., "The flow over a cylinder with various nose shapes at zero angle of attack at hypersonic speeds," Aeronaut. Res. Lab. 63-14 (January 1963).

## Thermal Conductivity of Gaseous Unsymmetrical Dimethylhydrazine

ROBERT D. ALLEN\*

Dynamic Science Corporation, South Pasadena, Calif.

The thermal conductivity of gaseous unsymmetrical dimethylhydrazine was determined by a modified hot-wire technique employing five standard gases. Data were obtained at average temperatures of about 5°, 10°, 30°, and 35°C. All gases were run at a pressure of  $\frac{1}{5}$  atm in order to overcome convection effects. Assuming linearity with temperature, the thermal conductivities were  $266 \times 10^{-7}$  and  $316 \times 10^{-7}$  cal/cm-sec-°C at 0° and 50°C, respectively.

IN the hot wire method, a gas at specified temperature and pressure is admitted to a long, narrow cylinder whose axis coincides with a thin wire. This wire is electrically heated by a stable d.c. power supply to a temperature slightly higher than that of the cylinder wall. The temperature difference must be large enough to allow accurate measurement but not so great as to produce large variations in gaseous thermal conductivity between wire and wall. The resistance of the wire as a function of temperature is known, so that resistance measurements determine wire temperatures. The temperature of the cylinder wall is maintained at a preselected value by immersion in a constant temperature bath. Heat flow rate from wire to wall is calculated from the amperage and voltage drop along the test length. The wire should be thin enough to approximate semi-infinite length; this geometry produces a long constant-temperature test section.

The total heat flow rate from the constant temperature section of the heated wire to the cylinder wall is given by the equation

$$Q_t = JEI = Q_k + Q_c + Q_r \quad (1)$$

where  $J$  is a conversion constant,  $E$  voltage drop along the test section,  $I$  amperage through the circuit,  $Q_k$  heat flow rate due to conduction,  $Q_c$  heat flow rate due to convection, and  $Q_r$  heat flow rate due to radiation.

A previous investigator<sup>1</sup> has reported that convection effects are minimized by orienting the test cylinder in vertical position. Findings in the present study have verified this conclusion. Convection is nearly eliminated by testing at reduced pressure; at 1 atm, 2.5% of the heat transfer was attributable to convection, whereas at  $\frac{1}{5}$  atm, convective heat transfer was negligible. Likewise, heat transfer by radiation is very small if the filament area is low and if the temperature drop from filament to cylinder wall is not large.

Received May 6, 1963. The investigation reported in this paper was supported by Lockheed Missiles and Space Company, Sunnyvale, Calif., as part of a program to study the forces on propellants due to heat transfer. The cognizant Lockheed program supervisor was Hugh M. Satterlee.

\* Senior Engineer.

Low emissivity surfaces of filament and wall reduce radiant heat transfer to a very insignificant percentage of the total heat flow rate. In the present apparatus, only about 0.05% of the heat was transferred by radiation.

Thus, the terms  $Q_e$  and  $Q_r$  in Eq. (1) can be dropped and the expression written in the form

$$Q_t = JEl = \frac{2\pi kl(t_1 - t_2)}{\ln r_2 - \ln r_1} \quad (2)$$

where  $k$  is thermal conductivity,  $l$  length of test section,  $t_1$  temperature of the wire,  $t_2$  temperature of the cylinder wall,  $r_1$  radius of the wire, and  $r_2$  inner radius of the cylinder wall.

It is essential to consider four other possible systematic errors: 1) inaccuracy in measurement of temperature at the cylinder wall; 2) loss of heat by conduction from the ends of the wire; 3) inaccuracy in resistance vs temperature calibration of the filament; and 4) temperature drop between the filament and the adjacent gas. The temperature of the internal cylinder wall was considered equivalent to the temperature of the liquid medium in which the cylinder was immersed; calculations based upon experimental heat flow rates and the thermal conductivity of brass showed that temperature drop through the cylinder wall was of the order of 0.004°C, less than one-half of the observational error of thermometer readings. Calculations showed that rate of heat loss by conduction from the ends of the wire was a very small percentage of the total heat flow rate; even this small loss would be compensated by use of standard gases.

On the other hand, inaccuracy in wire calibration and the temperature discrepancy between wire and adjacent gas molecules singly or together can produce large errors. These difficulties can be overcome readily by use of a series of standard gases of differing molecular weights and known thermal conductivities. Since both systematic errors affect the conductivity equation by producing an incorrect determination of  $t_1 - t_2$ , the standardizations are conducted to determine a calibration factor in order to correct this measured temperature difference. Equation (2) can be rewritten as

$$k = Q_t / A\alpha(t_1 - t_2) \quad (3)$$

where  $A$  is equal to  $2\pi l / \ln r_2 - \ln r_1$ , and  $\alpha$  is the calibration factor. The calibration factor is a function of both molecular weight of the gas and experimental environment. Thus, for each combination of bath temperature and power level used, it is necessary to establish a calibration curve of  $\alpha$  vs molecular weight. The thermal conductivity of a test gas thus is calculable from the experimental heat flow rate  $Q_t$ , experimental temperature difference  $t_1 - t_2$ , and the value of  $\alpha$  for the molecular weight of the test gas under the conditions imposed.

### Experimental Equipment and Procedures

A 1-in.-diam brass rod was used for the main body of the thermal conductivity test cell and for threaded caps at either end. An axial hole  $0.200 \pm 0.0015$  in. in diameter and 8 in. long was drilled to provide the desired internal geometry of the cell. End caps were sealed with teflon gaskets. The brass rod was machined in such a manner that a flat area was preserved tangent to the axial hole at either end. Teflon-insulated positioning plates were mounted on these flat areas to permit accurate location of a platinum wire filament of 0.001 in. diam coincident with the hole axis. From each positioning plate, an electrical lead was carried to its exit point through an epoxy seal. At the exit point, each lead was conducted through a glass tube to prevent contact with the water bath; preliminary experiments had shown that electrically hot leads in contact with even distilled water can produce large galvanic effects. The brass end cap at the upper end of the cell was soldered to a  $1\frac{3}{8}$ -in. length of stainless steel tubing that connected with the gas system. All brass components were gold plated to minimize chemical

corrosion. The platinum filament was calibrated by measuring its initial resistance to the passage of direct current when it was immersed in distilled water at measured temperatures.

All components in the gas system were fabricated from 316 stainless steel. These consisted of the following: 1) an admittance valve; 2) a 1-liter capacity mixing chamber (primarily for conductivity experiments involving more than one gas); 3) a 0- to 30-in. vacuum gage; 4) a two-way valve connecting the mixing chamber with both vacuum line and conductivity test cell; and 5) appropriate connecting lengths of threaded stainless steel tubing. The system was evacuated with a mechanical vacuum pump. A U-tube filled with glass wool was immersed in liquid nitrogen to trap gaseous unsymmetrical dimethylhydrazine and thereby minimize corrosion of the pump.

The electric power for heating the platinum filament was supplied by a 12-v battery. The voltage was stabilized with a single-stage transistorized control circuit that employed a Zener diode as reference element. A variable resistance provided desired variations in voltage. The output of the control circuit was passed in series through a standard 40-ohm resistor and through the filament of the conductivity cell. A Leeds and Northrup no. 7645 potentiometer was used to measure the voltage drops across the cell and standard resistance, respectively.

A large Dewar, with stirrer and accurate mercury thermometer, was employed as constant temperature bath for the cell. Experiments were conducted at environmental temperatures of approximately 0° and 25°C. At each temperature, potential drops of about 1.15 and 1.45 volts were imposed on the 40-ohm resistor. The apparatus successively was evacuated and filled with the test gas until extraneous gases had been reduced to negligible concentrations. When thermal equilibrium had been established, at least 10 successive readings were taken of bath temperature, cell voltage, and standard resistor voltage. Whenever a systematic change in either voltage occurred, readings were withheld until thermal equilibrium was re-established; very small changes in bath temperature or dry-cell output were reflected immediately by such changes. The potentiometer was standardized before each group of similar readings.

The following standard gases were employed: helium, nitrogen, argon, carbon dioxide, and acetone. All runs were conducted at  $\frac{1}{3}$  atm or slightly below.†

### Data Reduction

Total heat flow rate  $Q_t$  was calculated from the equation

$$Q_t = 0.005975 E_1 E_2 \quad (4)$$

where the coefficient is the conversion constant  $J$  divided by the standard resistance of 40 ohms, and  $E_1$  and  $E_2$  are the respective voltages across filament and standard resistor. Resistance of the filament was calculated from the equation

$$R_1 = 40 E_1 / E_2 \quad (5)$$

Temperature of the filament in degrees Centigrade was calculated from the following analytical expression of the experimental temperature-resistance curve:

$$t_1 = R_1 - 35.84812 / 0.11894 \quad (6)$$

Standard gas data were substituted into Eq. (3) to obtain values of  $\alpha$ , the calibration factor. Thermal conductivities for the standard gases were obtained by interpolation from Refs. 2 and 3. The standard conductivities first substituted into Eq. (3) applied to temperatures  $t_1 + t_2/2$ . These were somewhat too high, since the true gas temperature at the

† Unsymmetrical dimethylhydrazine was manufactured by Chlor-Alkali Division of Food Machinery and Chemical Corporation, New York.

**Table 1 Thermal conductivities of gaseous unsymmetrical dimethylhydrazine**

|   | $k, (\text{cal-cm}^{-1}\text{-sec}^{-1}\text{-}^\circ\text{C}^{-1}) \times 10^7$ | $T, ^\circ\text{C}$ |
|---|--|---------------------|
| Experimental  | 272  | 5.7                 |
|   | 274  | 9.2                 |
|   | 293  | 29.5                |
|   | 301  | 33.1                |
|   | 266  | 0                   |
| Calculated<br>(on basis of<br>linear variation<br>with temperature) | 276  | 10                  |
|   | 286  | 20                  |
|   | 296  | 30                  |
|   | 306  | 40                  |
|   | 316  | 50                  |
|   |  |                     |

filament was always less than the filament temperature. Therefore, the first values of  $\alpha$  calculated were used to estimate the true gas temperatures at the filament from Eq. (7):

$$\alpha = \Delta t(\text{true})/\Delta t(\text{experimental}) \quad (7)$$

Thermal conductivities then were adjusted downward to conform to the average temperatures  $t_{g(1)} + t_2/2$ , where  $t_{g(1)}$  denotes the first calculated temperature of the gas at the filament. This procedure was repeated until calculated values of  $\alpha$  converged.

Calibration curves of  $\alpha$  vs molecular weight of standard gas were plotted for the four experimental environments used: 1) minimum voltage,  $0^\circ\text{C}$  bath; 2) maximum voltage,  $0^\circ\text{C}$  bath; 3) minimum voltage, room temperature bath; and 4) maximum voltage, room temperature bath. Thermal conductivities for unsymmetrical dimethylhydrazine were calculated from Eq. (3) by selecting the values of  $\alpha$  appropriate to its molecular weight of 60.08 and each experimental environment. (The value of  $\alpha$  varied from 0.655 to 1.025). The mean temperature applicable to each thermal conductivity was given by

$$\langle t \rangle = t_2 + [\alpha(t_1 - t_2)/2] \quad (8)$$

### Results

Thermal conductivities of gaseous unsymmetrical dimethylhydrazine are presented in Table 1. On the basis of linear variation with temperature, the change in thermal conductivity with respect to change in temperature,  $\Delta k/\Delta T$ , is very close to  $10^{-7}$  cal/cm-sec- $^\circ\text{C}^2$ .

### References

- 1 Archer, C. T., "Thermal conduction in hydrogen-deuterium mixtures," *Proc. Roy. Soc. (London)* **A165**, 474-485 (1938).
- 2 McAdams, W. H., *Heat Transmission* (McGraw-Hill Book Co. Inc., New York, 1954), 2nd ed., p. 391.
- 3 Forsythe, W. E., *Smithsonian Physical Tables* (Smithsonian Institution, Washington, D. C., 1954), 9th revised ed., p. 142.

## Second Approximation to the Solution of the Rendezvous Equations

HOWARD S. LONDON\*

United Aircraft Corporation, East Hartford, Conn.

The equations of motion of a satellite relative to a coordinate system whose origin moves in a circular satellite orbit are solved to second order by the method of successive approximations. The closed-

form solution thus obtained provides a second-order correction to the standard linear solution and, on the basis of sample cases representative of rendezvous conditions, appears to decrease greatly the numerical errors resulting from the use of the linear solution alone.

THE familiar linear approximation to the solution of the equations of relative motion of a satellite moving in a circular orbit and a nearby satellite has been used extensively in studies of rendezvous operations, e.g., Refs. 1 and 2. It has been recognized, however, that the numerical accuracy of the linear solution is not adequate for many cases of interest.<sup>3</sup> Errors that increase with flight time result from neglecting second- and higher-order terms in various components of relative distance (range) and relative velocity (range rate) normalized with respect to orbital radius and orbital velocity, respectively, depending upon the particular coordinate system used.<sup>4</sup>

Since the range and range rate are small in most cases of current interest, it is felt intuitively that the accuracy of the linear solution can be improved considerably by adding a second-order correction. The second-order correction in rectangular coordinates is obtained herein by the method of successive approximations, i.e., second-order gravitational terms are retained in the differential equations of relative motion and approximated by the results of the linear solution. These terms thereby become time-dependent forcing functions in a set of linear differential equations for the second-order correction; the solution is obtained in closed form as a function of time and the initial values of the components of range and range rate.

A rectangular coordinate system is chosen such that its origin moves in a circular orbit of radius  $r_0$  with the angular speed  $\omega$  corresponding to satellite speed at  $r_0$ ; the  $x$ - $y$  plane is in the plane of this orbit and the  $z$  direction normal to it. The equations of relative motion of a satellite are, in dimensionless form,

$$\ddot{x} - 2\dot{y} + x[(1/r^3) - 1] = 0 \quad (1)$$

$$\ddot{y} + 2\dot{x} + (1 + y)[(1/r^3) - 1] = 0 \quad (2)$$

$$\ddot{z} + (z/r^3) = 0 \quad (3)$$

$$r = (1 + 2y + x^2 + y^2 + z^2)^{1/2} \quad (4)$$

where  $x$ ,  $y$ ,  $z$ , and  $r$  are normalized with respect to the orbital radius  $r_0$ ;  $\dot{x}$ ,  $\dot{y}$ , and  $\dot{z}$  are normalized with respect to orbital velocity at  $r_0$ , and the dot notation indicates differentiation with respect to the dimensionless time  $\tau = \omega t$ . The term  $r^{-3}$  is expanded in a binomial series and terms of third order and higher in Eqs. (1-3) are dropped, giving equations that are correct to second order

$$\ddot{x} - 2\dot{y} - 3xy = 0 \quad (5)$$

$$\ddot{y} + 2\dot{x} - 3y + 3y^2 - \frac{3}{2}(x^2 + z^2) = 0 \quad (6)$$

$$\ddot{z} + z - 3yz = 0 \quad (7)$$

Now let  $x = x_1 + x_2$ ,  $y = y_1 + y_2$ , and  $z = z_1 + z_2$  where subscript 1 denotes the first-order solution and subscript 2 denotes a second-order correction. It is assumed that if terms in the first-order solution are of order of magnitude  $\delta$ , then terms in the second-order correction are of order  $\delta^2$ . Accordingly, the first-order equations are

$$\ddot{x}_1 - 2\dot{y}_1 = 0 \quad (8)$$

$$\ddot{y}_1 + 2\dot{x}_1 - 3y_1 = 0 \quad (9)$$

$$\ddot{z}_1 + z_1 = 0 \quad (10)$$

and the equations for the second-order corrections, consistent with the order-of-magnitude assumptions, are

$$\ddot{x}_2 - 2\dot{y}_2 = 3x_1y_1 \quad (11)$$

Received January 14, 1963.

\* Research Engineer, Research Laboratories. Now Member of the Technical Staff, Bellcomm, Inc. Member AIAA.